Magazine of Civil Engineering

ISSN 2712-8172

journal homepage: http://engstroy.spbstu.ru/

Research article

UDC 627.52

DOI: 10.34910/MCE.120.8

Sedimentation simulation of the Temryuk seaport approach channel

I.G. Kantardgi [1], ***I.O. Leont'yev*** [2], ***A.V. Kuprin*** [1] ✉

[1] *Moscow State University of Civil Engineering (National Research University), Moscow, Russian Federation*

[2] *Shirshov Institute of Oceanology, Russian Academy of Sciences, Moscow, Russian Federation*

✉ *rtyter55@gmail.com*

Keywords: longshore sediment transport, erosion, drift, accumulation, protective measures, mathematical model

Abstract. The sedimentation of the approach channel and the water area of Temryuk port is an important problem that has recently attracted the attention of researchers and engineers. The object of the study is the influence of the extension of the east and west breakwaters of the port. An analytical method of forecasting lithodynamic processes for various extensions of protective breakwaters was used. To verify the results, an analysis of space images of the coastal zone was applied. The volumes of sedimentation of the sea part of the Temryuk port approach channel were determined; recommendations for the extension of breakwaters were given. The sedimentary layer in the Temryuk Bay has two demarcated zones, one dominated by silty material, and the other, coastal, by fine-grained sand. Therefore, to determine the total alongshore sediment flow, the movement of muddy and sand flows was determined separately. The west breakwater retains only a small part of the sand transported to the canal; the east breakwater also has an insufficient length. The majority of the sand passing in the west and east directions falls into the canal. After the extension of the east breakwater by 100 m, the sedimentation of sand will be due mainly to its arrival from the west side, and thus the maximum thickness of the sediment layer will be about 2 m. The extension of the east breakwater by 200 m does not lead to a significant improvement compared to the extension option of 100 m, therefore, to reduce the sedimentation, it is necessary to extend the west breakwater by 100 m as well. After the extension of the west breakwater, the flow of sand into the channel from the west side will be significantly reduced. Thus, after the lengthening of both breakwaters, the volume of sedimentation of the channel with sand will decrease from 55 to 15 thousand cubic meters per year. The main contribution to the sedimentation will continue to be made not by sandy, but by silty material.

Citation: Kantardgi, I.G., Leont'yev, I.O., Kuprin, A.V. Sedimentation simulation of the Temryuk seaport approach channel. Magazine of Civil Engineering. 2023. 120(4). Article no. 12008. DOI: 10.34910/MCE.120.8

1. Introduction

Construction of protective structures at seaports is a classical way to protect the approach channel and water area from sedimentation and penetrating waves. However, in practice, the effectiveness of breakwaters as a protection against sedimentation decreases with the time of port operation. Sedimentation in the area of the unprotected approach channel approaches catastrophic levels. It is expressed in more rapid reduction of depths in the fairway at the port gates, as compared to the remote parts of the channel at sea. The most exposed to this type of sedimentation are port approach channels located on the shallow sandy shores of the Black, Azov and Baltic Seas with a developed longshore sediment flow.

Enclosing west and east breakwaters are located in the port of Temryuk, Krasnodar region, Temryuk district, Temryuk Bay of the Azov Sea (Fig. 1). The approach channel of Temryuk seaport was built in 1910 for navigational safety of vessel passage.

Figure 1. Location of the investigated breakwaters of Temryuk port, Russia (breakwaters are highlighted in red).

A serious problem of Temryuk port geographical location is its proximity to the mouth of the Kuban River. Solid flow of the Kuban River determines morphodynamic changes in the coastal zone, including a significant sedimentation of the approach channel of Temryuk port by sand and silt deposits.

Observations and experimental studies in a number of ports [1, 2] revealed the sedimentation characteristics of approach channels protected by barrier structures. The construction of breakwaters divides the coastal zone into two regions with a different dynamic activity of waves, currents and sediment transport. As a result of the interruption of longshore sediment flow, large volumes of bottom sediments rapidly accumulate at the root of the windward mole (Fig. 1). This form of filling the incoming angle with sediment, followed by downstream erosion of the section of coast behind the leeward breakwater, is most relevant to port construction.

Previous work on the subject was analysed in the preparation of this paper. Papers [3–6] provide material on the modelling of longshore sediment transport. Information on the comparison of different approaches to the determination of longshore sediment transport rates is given in [7]. The papers [8, 9] discuss new models for predicting shoreline changes: a model based on the dynamic coupling of a high-resolution one-dimensional cross-shore model to a two-dimensional area model for calculating the total longshore sedimentation rate; a model based on machine learning techniques. A new method for verification of beach dynamics predictions was developed in [10].

One of the goals of this work is to estimate the possible volumes of sediment accumulation in the approach channel to the port of Temryuk, considering the general lithodynamic situation in the adjacent area. We are talking about the marine part of the channel, where the main factors of sedimentation are waves and associated currents that generate longshore sedimentations, which deliver the material to the channel bed.

The second goal of the work is to develop recommendations for extending the breakwaters enclosing of the coastal part of the channel on the east and west sides. The extension of the breakwater should reduce the sedimentation of the channel. However, the considerable cost of the structure imposes restrictions on the choice of its optimal length.

The mentioned problems are investigated in the present work on the basis of mathematical modelling of coastal lithodynamic processes [11–18].

At present, all-Russian and departmental normative documents on the design of approach channels [19] do not contain recommendations for determining the volume of catastrophic sediment deposition and methods for preventing it. Existing software complexes for determining the volume of approach channel sedimentation have certain drawbacks.

The existing normative base for design of sea approach channels is outdated and requires updating. A number of recommendations of all-Russian and departmental normative documents do not meet the requirements of modern design practice. They are developed on the models, which do not correspond to

the modern level of knowledge about hydrolytodynamics of the coastal zone. The norms of design of sea approach channels do not contain recommendations, in which the initial data would include the parameters of engineering geology and coastal hydrolytodynamics. The sedimentation reserves are set depending on the dimensions of the design vessel. The phenomenon of sedimentation is accounted for by an empirical coefficient. In the process of designing, incorrect decisions lead to unjustifiably high volumes of repair dredging, and, consequently, to significant financial costs. In this connection, investigation of the process of sedimentation of the approach channels and the ways of its prevention is an actual problem.

Analysis of baseline information confirms high, constant sedimentation of the approach channel, which leads to the need for regular repair clearing of the channel and the port water area. Thus, according to FSUE Rosmorport, the volume of repair dredging was 129406.2 m^3 in 2020 and 120102.4 m^3 in 2021.

At the same time, sedimentation ability of the approach channel varies significantly along its length. According to the passport of approach channel, its sedimentation varies from 10 cm per year, to 100 cm and more per quarter.

Maximum sedimentation occurs in the head part of the east breakwater, both in the direction to the sea part of the channel and to the port part of the channel.

Simultaneously with sedimentation of the channel, the incoming angle for the east breakwater is filling up with shoreline advance into the sea. The rate of shore advance near the breakwater during the first year after its construction is about 50 m. The process of shore advancement from the inlet corner of the east breakwater directly affects the sedimentation of the approach channel, since after the shore reaches the head of the breakwater, the sediment will be transported by the longshore current directly into the channel.

According to survey data, the sedimentation of the approach channel occurs by storms from the east and west directions, the main sediment flow occurs from the east direction.

The main objectives of the work are:

1) Study of lithodynamic regime of the area under consideration in natural (modern) conditions.

2) Forecast of sedimentation of the approach channel of the seaport for several proposed variants of the east and west breakwater extension and selection of the extension option that provides an acceptable level of sedimentation.

2. Methods

An important feature of the sediment layer on the bottom in the studied area of the Azov coast, Russia (Temryuk Bay) is the existence of two rather clearly delineated zones, one of which (at depths greater than 3 m) is dominated by silty material, while the other, coastal (at depths less than 3 m) is dominated by fine-grained sand. This leads to the need to model separately the flows of sandy and muddy sediments when determining the total longshore flow. It should be noted that existing methods focus mainly on sandy sediments. In order to obtain estimates with respect to silt transport, it was necessary to develop a special calculation methodology.

2.1. Sandy sediment

The methodology for calculations concerning sandy sediments is outlined, for example, in [17, 20–26]. The basic formula for determining the local longshore sand discharge q under the action of waves and the accompanying current, expressed in $m^3m^{-1}h^{-1}$:

$$q = \mu\left[\frac{9\pi}{8}\frac{\varepsilon_b}{\tan\alpha_g}\frac{D_f}{u_m} + \frac{\varepsilon_s}{w_g}\left(4D_f + B\right)\right]V_b. \quad (1)$$

Here $\mu = 3600\Big/\left[g\left(\rho_g - \rho\right)\left(1-\sigma\right)\right]$ is the coefficient, which agrees dimensions, g is acceleration of gravity, ρ and ρ_g are densities of water and solid particles, σ and α_g are porosity and angle of natural slope of ground, ε_b and ε_s are efficiency coefficients of transport of bedload and suspended sediments (0.1 and 0.02 respectively), u_m is amplitude of orbital wave velocity near the bottom, $D_f = \frac{2}{3\pi}\rho f_w u_m^3$ is energy dissipation rate due to bottom friction, f_w is coefficient of bottom friction for waves, w_g is sedimentation rate of solid particles (hydraulic coarseness), B value accounts for additional energy

dissipation in the bottom layer due to turbulence penetration from surface layer at wave collapse, V_b is bottom velocity of longshore current. The latter is related to the depth-averaged current velocity $\bar{V}$ as $V_b = \bar{V} / \left[\ln\left(h / z_a\right) - 1 \right]$, where h is depth and z_a is the apparent roughness of the bottom for the current. The value $\bar{V}$ is calculated using the equations of hydrodynamics, and Snell's law of refraction and the energy balance equation are used to calculate refraction, transformation, and wave energy dissipation.

2.2. Slimy sediments

Unlike sand, physical properties of silty sediments change in time and depend on dynamic conditions. Thus, to set in motion a layer of silt formed relatively recently (days, weeks), a flow velocity of about 0.2 m*s^{-1} is sufficient, and to move the sediment particles that have been at rest for a long time (months, years) a speed of about 1 m*s^{-1} is required. It is also known that under the influence of waves the threshold of touching for silty soils is much lower, since periodic pressure changes in the pores lead to weakening of particles adhesion. According to the data given by Van Rijn [27] the wave action on low compacted clayey soil starts the movement of the material at bottom tangential stress τ_m > 0.2 N*m^{-2}. Even relatively small waves can create an appreciable flow of muddy material.

In contrast to the sandy bottom, the current above the silt layer acts in a smooth regime, the roughness parameter is characterized by a value of less than 1 mm. Accordingly, the friction coefficient is significantly reduced.

Considering the fact that the sludge is mainly transported in suspension, its flow rate q', based on formula (1), can be expressed as

$$q' = 4\mu\alpha_w D_f V_b, \quad \alpha_w = \frac{\varepsilon_s}{w_g} \tag{2}$$

(B is neglected, assuming that the muddy sediments lie outside the collapse zone). The main problem is the estimation of the parameter α_w. In the case of sand, the efficiency factor ε_s is estimated to be 0.02, the settling velocity w_g for fine sand is of the order of 10^{-2} m*s^{-1}, and the value of α_w is close to unity. For silt, due to the bonding forces between particles, the value of ε_s should probably be lower than for sand. However, the solids deposition rate w_g is also significantly lower here. The order of magnitude of α_w for silty soil can only be estimated from experimental data.

Let us express flow q' in units of dry mass (in kg m^{-1}s^{-1}), rewrite formula (2) in terms of bottom tangential stress τ_m and pass from flow to depth average suspended solids concentration C (kg/m^3), connected with flow as $C = \frac{q'}{hV_b}$. Keeping in mind that in wave flow $D_f = \frac{4}{3\pi}\tau_m u_m$, where $\tau_m = \frac{1}{2}\rho f_w u_m^2$, we obtain from (2)

$$\begin{gathered} q' = \frac{16}{3\pi}\frac{\rho_g}{\left(\rho_g - \rho\right)}\alpha_w \tau_m u_m V_b, \\ C = \frac{16}{3\pi}\frac{\rho_g}{\left(\rho_g - \rho\right)}\frac{\tau_m u_m}{gh}\alpha_w \cong 3.4\frac{\tau_m u_m}{gh}\alpha_w, \end{gathered} \tag{3}$$

where the numerical coefficient in the last ratio corresponds to the typical value of the density of mud particles ρ_g = 2×10^3 kg/m^3.

To estimate the value of α_w, the data on suspended sediment concentration obtained in [28] can be used. The measurements were made both in a wave basin and in full-scale conditions (in the coastal zone of the Yellow Sea). The observation conditions and obtained estimates of α_w values are shown in

Table 1. The depths h, significant heights H_s and corresponding wave periods T_s, as well as the values of concentration C are shown here.

In the calculations it was assumed that under smooth bottom conditions the coefficient of friction is close to the values of f_w = 0.01. The obtained values of α_w have quite a large scatter, but in general of the same order. In the first approximation it is possible to accept the averaged estimation α_w = 2.8, on which further calculations of sediment flow using formula (2) will be based.

Table 1. Measurement conditions of sludge suspended solids concentration in laboratory and marine conditions [20] and calculated estimates of parameter α_w.

h, m	H_s, m	T_s, s	C, kg/m^3	α_w, s m^{-1}
Wave Pool				
0.1	0.075	1.2	0.5	1.8
0.1	0.050	2.2	0.2	2.5
0.1	0.035	1.2	0.05	1.7
Marine conditions				
5	2	8	0.65	2.4
5	1.5	8	0.55	4.8

2.3. The amount of accumulation in the channel

Some of the sediment passes over the channel by transit. Therefore, it is necessary to estimate how much of the material falls to the bottom and contributes to the sedimentation. In this case, the well-known Galvin dependence is used for this purpose [29]:

$$Ac = q\left[1-\left(\frac{h}{h_c}\right)^2\right], \tag{4}$$

where Ac is the local rate of sediment accumulation in the channel (per meter of length), q is the longshore flow rate of sediment in front of the channel, h is the natural depth, h_c is the depth in the channel. The deeper the channel is relative to the natural depth, the more sediment it absorbs.

3. Results and Discussion

The bathymetric basis for modelling is a navigation map of scale 1:10000, as well as survey data in the vicinity of the channel. The isobath plan in the Temryuk port area is shown in Fig. 2. The general direction of the coastline in the area under consideration is close to the west-east direction.

As mentioned above, at depths less than 3 m the bottom is covered by a layer of fine sand with shell fragments averaging 0.15 mm, while deeper than 3 m there is silt. The bottom within the sandy layer has a slope of about 0.01, and more narrowly the slopes decrease to values of 0.002–0.005.

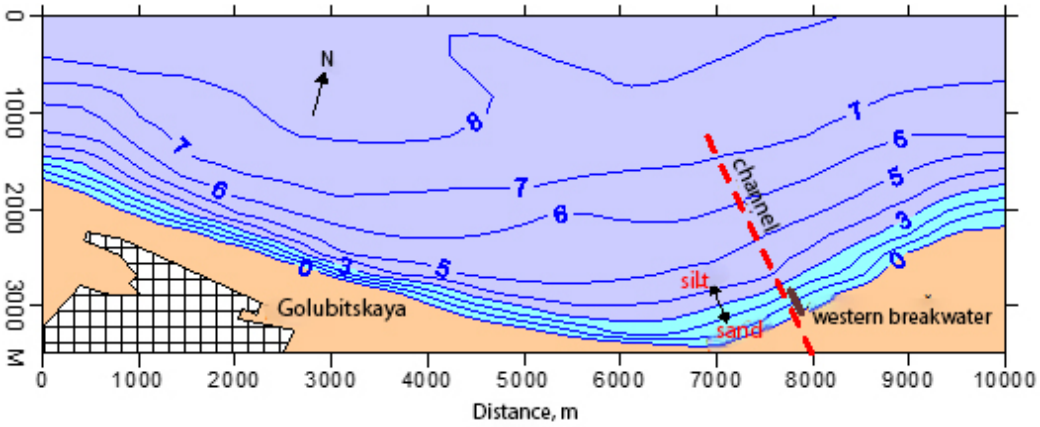

Figure 2. Bottom bathymetry in the channel vicinity.

The position of the existing structures at the mouth of the channel is reflected in Fig. 2. The east breakwater currently terminates at a depth of 1 m and thus allows sandy sediments to flow into the channel at depths of 1 to 3 m. The depth at the end of the west breakwater is only about 0.5 m, and the longshore flow of sediment created by the waves of the west channels is almost unimpeded into the channel.

The length of the offshore part of the channel from the beginning in the open sea to the head of the east breakwater is 2,700 m. The channel floor width varies from 95 to 100 m. The design depth in the channel varies from 6.4 to 6.9 m. The deepest part is before the end of the east breakwater. During calculations, the depth of the channel was assumed to be 6.9 m.

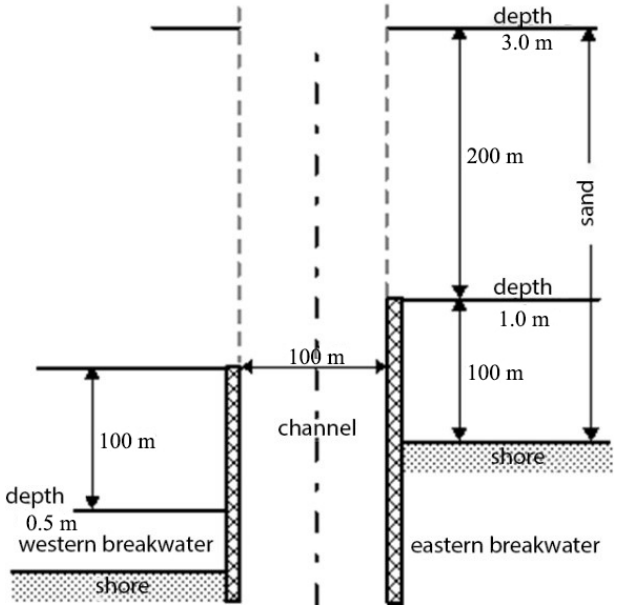

Figure 3. Diagram of the shoreline at the mouth of the channel.

The wave pattern in the Temryuk coastal area is characterized by the predominance of the NE direction. The wave mode is shown in Table 1, based on data from the Russian Maritime Register of Shipping [30].

Table 2. Annual duration of waves of different strengths for the main directions.

H_s, m	T_s, s	t_w, h			
		W	NW	N	NE
		Θ = 85°	Θ = 40°	Θ = –5°	Θ = –50°
0.6	3.6	429	473	394	929
1.0	4.2	184	158	131	464
1.3	4.7	53	35	26	166
1.8	5.0	8.8	6.1	3.5	44
2.1	6.0				7.0

Here is the total annual duration of waves (t_w) of different strength for the main wave directions (H_s and T_s are the significant height and corresponding period of waves in the open sea, Θ are the angles of approach of waves relative to the coastal normal).

3.1. Modelling of longshore sediment flows

The calculated distributions of the volumes of sand and silt moving over the profile of the coastal slope during the year are shown in Fig. 4. Separately, the westward and eastward flows created by the eastward and westward waves, respectively, are shown. As can be seen, the resultant flows are directed westward. The sandy sediment flow peaks closer to the water's edge at 1–2 m depths, while the silt flow peaks near the upper boundary of its distribution. The maximum values of sand fluxes in the near-river zone reach 200–400 cubic meters per meter of profile length per year. The peaks of flows to the west and to the east are shifted relative to each other due to the unequal position of the coastline on both sides of the channel (Fig. 3).

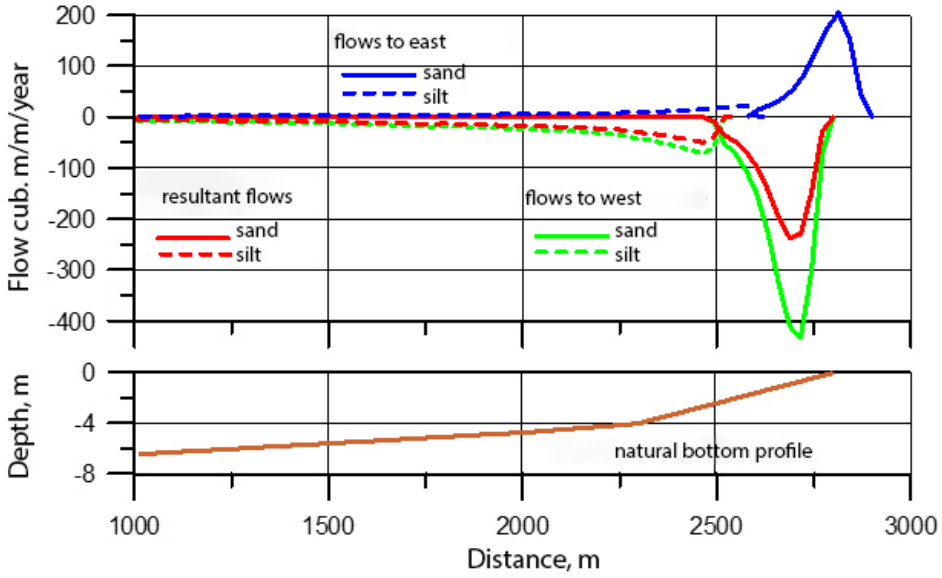

Figure 4. Distribution of longshore sediment fluxes along the profile of the coastal slope.

At depths greater than 3 m, only muddy sediment moves (at a peak of about 75 $m^3m^{-1}yr^{-1}$). Although the silt flows subside with increasing depth, the movement of material can be traced throughout the channel.

An idea of the integral material flows is given in Table 3. About 40,000 cubic meters of sand and silt move in the east direction per year, and about 100,000 cubic meters in the west direction. The resulting flow is westward and is about 60 thousand cubic meters per year, and the contributions of sand and silt are comparable.

Table 3. Integral longshore sediment flows (thousand cubic meters per year).

Flow	Sand	Silt
On east	27.2	9.4
On west	–58.8	–37.8
Totally	–31.6	–28.4

3.2. Channel sedimentation under existing conditions

The results of calculations of specific sediment accumulation (per meter of channel length) are shown in the upper graph of Fig. 5. The accumulation of sand is characterized by two peaks. The smallest and closest peak is associated with the westward rumb waves (209 m^3m^{-1} $year^{-1}$). The second and largest peak (440 m^3m^{-1} $year^{-1}$) is due to the eastward waves. It is displaced towards the sea, as part of the flow is blocked near the coast by the east breakwater. As for the silt, it is deposited mainly at depths of 3 to 5 m (in the peak up to 75 m^3m^{-1} $year^{-1}$ at 3 m depth).

Specific channel sedimentation is also presented as Table 4. The distance between pickets is 100 m, they are counted from the end of the east breakwater towards the sea. Picket №-1 is located at the distance between the west and east breakwaters (Fig. 3).

Table 4. Accumulation of sediment in the channel at the existing conditions.

No range	Accum., m^3m^{-1} $year^{-1}$	No range	Accum., m^3m^{-1} $year^{-1}$	No range	Accum., m^3m^{-1} $year^{-1}$
-1	209	9	10	19	0.2
0	440	10	9.0	20	0.0
1	140	11	7.1	21	0.0
2	75	12	5.6	22	0.0
3	50	13	4.4	23	0.0
4	33	14	3.3	24	0.0
5	24	15	2.6	25	0.0
6	19	16	1.9	26	0.0
7	15	17	1.2	27	0.0
8	13	18	0.7		

The middle graph of Fig. 5 shows the distribution of conditional thickness of sediment layer Δh along the length of the channel (quotient of specific accumulation volume divided by the width of the channel). At depths less than 3 m, the thickness of sand sediment layer can reach 4 m per year. Maximum silt layer up to 0.7–0.8 m per year is observed at a depth of about 3 m (near the conventional boundary between sand and silt). With the distance from the shore the thickness of accumulation layer decreases and at the depth of more than 5 m the value of Δh becomes less than 0.2 m.

Integral indices of channel sedimentationing and accumulation near moles are shown in Table 5. Total volume of channel sedimentationing is estimated as 78 thousand m^3/year, 70 % of which is caused by sand.

The west breakwater retains only a small part of the sand transported to the channel (3 thousand m^3/year). The east breakwater, apparently, also has insufficient length and retains only 24 thousand m^3/year. Most of the sand passing in the west and east directions enters the channel (55 thousand m^3/year).

Table 5. Accumulation at the breakwaters and in the channel (thousand cubic meters per year) at the existing breakwaters.

Material	W breakwater	E breakwater	Channel
Sand	3.2	24.3	55.1
Silt	-	-	23.1

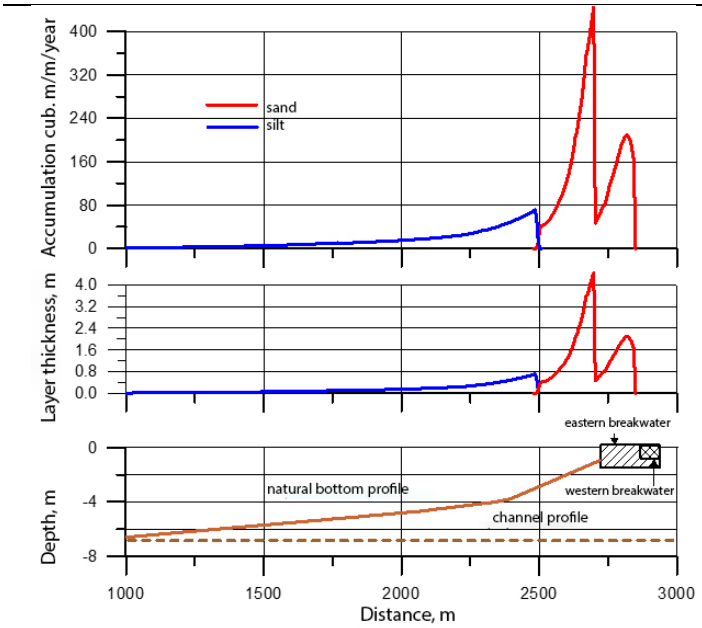

Figure 5. Distribution of the volume of sedimentation and thickness of sediment in the channel along the profile of the bank slope.

It should be noted that a certain part of sand can move along the breakwater and eventually end up in the channel as well. This is evidenced by the results of modelling of storm bottom deformations in the area of the channel mouth under NE storm conditions (Fig. 6). As can be seen, an accumulative sand body is formed near the head of the breakwater, which can be later moved into the channel. Thus, the local sedimentation here may exceed the values given above.

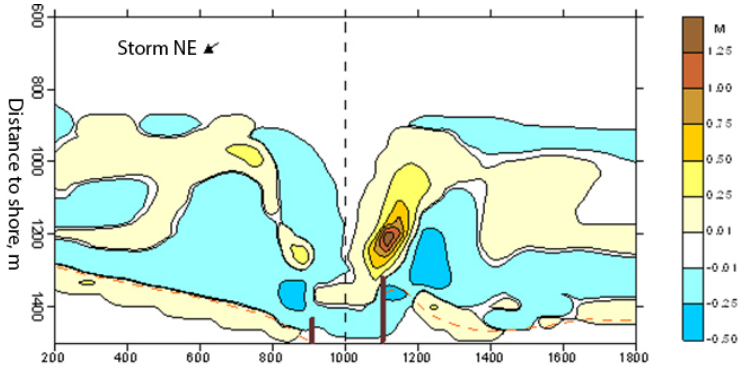

Figure 6. Storm deformation in the area of the channel mouth during the NE storm. Accumulation is highlighted in yellow and brown.

3.3. Options for extending the east breakwater

Based on the results obtained and the planned service life of the structures (class III – 50 years), two options for extending the east breakwater are considered.

Variant 1 assumes extension by 100 m. In this case, after 25 years, the situation with sedimentation will be approximately the same as it is at present. Namely, the presently existing section of the breakwater will be reached by the extending coastline. And about 100 m of the breakwater will provide protection.

Variant 2 assumes an extension of 200 m from the present position. In this case, the entire sandbar will be blocked. The sedimentationing will decrease and reach the present values only in 50 years.

Let's return to consideration of variant 1. If the breakwater is extended by 100 m, its length with respect to the current position of the shore will be 200 m, and the depth at the head will be about 2 m (Fig. 3).

The results of calculations of sedimentationing in variant 1 are shown in Fig. 7.

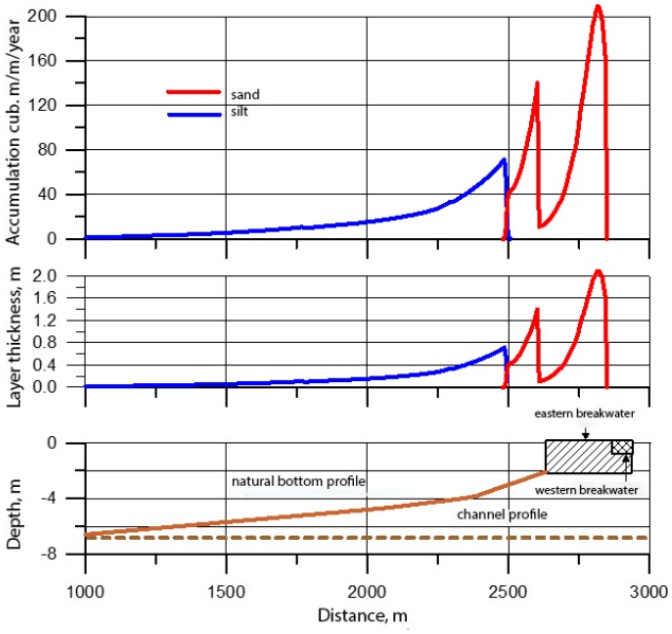

Figure 7 - Distribution of the channel skid volumes after extending the east breakwater by 100 m (variant 1).

As can be seen, the inflow of sand into the channel from the east side is markedly reduced (at a peak of 140 vs. 440 m^3m^{-1} $year^{-1}$ under the current position). The sand accumulation is now caused mainly by its inflow from the west side. The volume of silty sedimentation from the east side does not change.

The specific sedimentation of the channel in variant 1 is shown in Table 6, and the integral indices of sediment load and accumulation near the breakwaters are shown in Table 7. The east breakwater now retains twice as much sand. In total, about 30 thousand m^3 of sand per year enters the channel, which is almost twice less than under the existing situation (Table 5).

Table 6. Accumulation of sediment in the channel, variant 1.

No range	Accum., m^3m^{-1} $year^{-1}$	No range	Accum., m^3m^{-1} $year^{-1}$	No range	Accum., m^3m^{-1} $year^{-1}$
–1	209	9	10	19	0.2
0	43	10	9.0	20	0.0
1	140	11	7.1	21	0.0
2	75	12	5.6	22	0.0
3	50	13	4.4	23	0.0
4	33	14	3.3	24	0.0
5	24	15	2.6	25	0.0
6	19	16	1.9	26	0.0
7	15	17	1.2	27	0.0
8	13	18	0.7		

Table 7. Accumulation at the breakwaters and in the channel (thousand cubic meters per year), variant 1.

Material	W breakwater	E breakwater	Channel
Sand	3.2	50.3	30.2
Silt	-	-	23.1

The catching capacity of the east breakwater will gradually decrease over time, due to shoreline advance, which was noted in [19].

Variant 2. After extending the breakwater by 200 m, its length relative to the current position of the shore will be 300 m, and the depth at the head will be about 3 m (Fig. 3).

The results of calculations of sedimentationing in variant 2 are shown in Fig. 8. The enclosing breakwater now completely cuts off the inflow of sand on the east side. However, the sand sedimentation on the west side remains the same (more than 200 m^3m^{-1} $year^{-1}$, sediment thickness 2 m/year). The volume of sediment sedimentation is also unchanged.

Specific sedimentation of the channel in variant 2 is shown in Table 8, and the integral indices of sedimentation and accumulation near the breakwaters are characterized in Table 9.

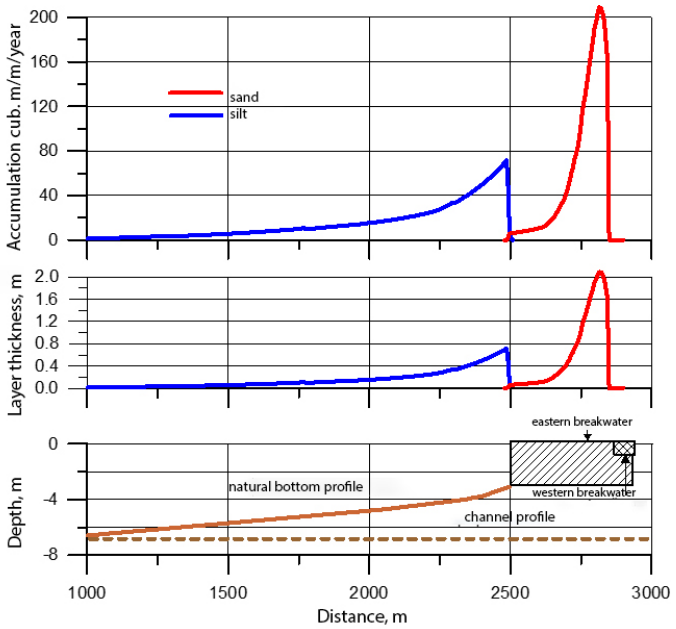

Figure 8. Distribution of channel skid volumes after extending the east breakwater by 200 m (variant 2).

Table 8. Accumulation of sediment in the channel, variant 2.

No range	Accum., m^3m^{-1} $year^{-1}$	No range	Accum., m^3m^{-1} $year^{-1}$	No range	Accum., m^3m^{-1} $year^{-1}$
-1	209	9	10	19	0.2
0	43	10	9.0	20	0.0
1	10	11	7.1	21	0.0
2	75	12	5.6	22	0.0
3	50	13	4.4	23	0.0
4	33	14	3.3	24	0.0
5	24	15	2.6	25	0.0
6	19	16	1.9	26	0.0
7	15	17	1.2	27	0.0
8	13	18	0.7		

Table 9. Accumulation at the breakwaters and in the channel (thousand cubic meters per year), variant 2.

Material	W breakwater	E breakwater	Channel
Sand	3.2	58.8	22.8
Silt	-	-	23.1

As can be seen, the sedimentation of sand in the channel is now a little less than 23 thousand cubic meters per year, which is only 7 thousand cubic meters less than in option 1. Consequently, Option 2 (extension of the breakwater by 200 m) does not result in a significant improvement over Option 1 (extension by 100 m). A more noticeable reduction in sedimentation can most likely be achieved by extending the west breakwater by the same 100 m.

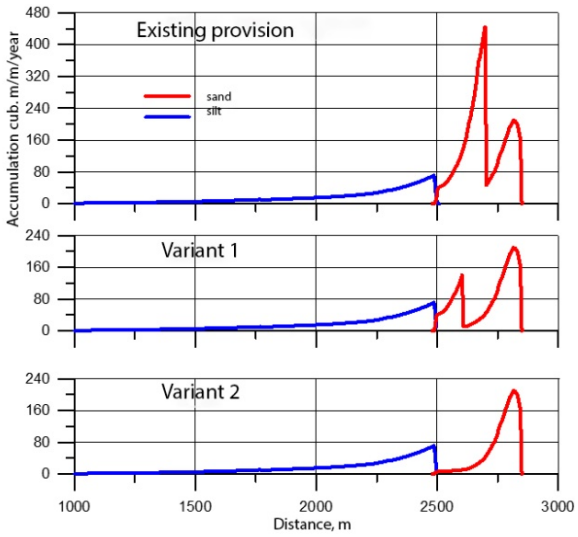

Figure 9. Distribution of channel skid volumes at different lengths of the east breakwater.

For the convenience of comparison, the channel sedimentation for different variants of the east breakwater is shown in Fig. 9. Variant 2, as compared to variant 1, removes the second peak of sand sedimentation on the east side, which is almost half the size of the sand sedimentation on the west side.

3.4. Channel sedimentation after extending the west breakwater

The distribution of the sedimentation after the extension of the west breakwater by 100 m is shown in Fig. 10. It is assumed that the east breakwater has already been extended by the same distance. The inflow of sand into the channel from the west side is now significantly less than before (at peak about 100 vs. 200 m^3m^{-1} $year^{-1}$ under the current position).

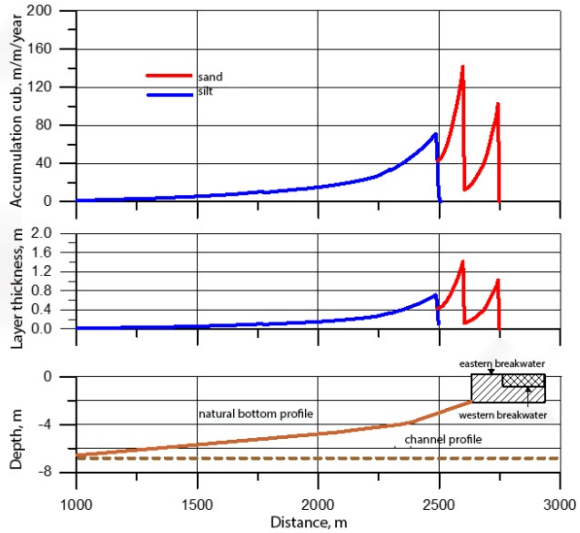

Figure 10. Distribution of the volume of the channel sedimentation after extending the west breakwater by 100 m (it is assumed that the east breakwater has already been extended by 100 m).

The specific sedimentation of the channel after extending the west breakwater is shown in Table 10, and the integral indices of sedimentation and accumulation at the breakwaters are characterized in Table 11. The west breakwater now retains 6 times more sand than before. In total, less than 15 thousand m^3 of sand per year enters the channel, which is half as much as before the west breakwater extending (Table 5).

Table 10. Accumulation of sediment in the channel after extending the west breakwater.

No range	Accum., m^3m^{-1} $year^{-1}$	No range	Accum., m^3m^{-1} $year^{-1}$	No range	Accum., m^3m^{-1} $year^{-1}$
-1	102	9	10	19	0.2
0	43	10	9.0	20	0.0
1	140	11	7.1	21	0.0
2	75	12	5.6	22	0.0
3	50	13	4.4	23	0.0
4	33	14	3.3	24	0.0
5	24	15	2.6	25	0.0
6	19	16	1.9	26	0.0
7	15	17	1.2	27	0.0
8	13	18	0.7		

Table 11. Accumulation at the breakwaters and in the channel (thousand cubic meters per year) after the extension of the west breakwater.

Material	W breakwater	E breakwater	Channel
Sand	19.9	50.3	14.6
Silt	-	-	23.1

Thus, after extending the breakwaters, the volume of sedimentation of the channel will decrease from 55 to 15 thousand cubic meters per year. As a result, the main contribution to the sedimentation will be made not by sand, but by silty material. It should be emphasized that the planned measures for extending the breakwaters have no effect on the volume of silty sediment accumulation, which spreads beyond the 3-meter isobath.

Distribution of sedimentation volumes at the existing position, at extension of the east breakwater only, as well as at extension of both breakwaters are compared in Fig. 11. Obviously, the latter option is the most preferable in terms of sedimentation reduction.

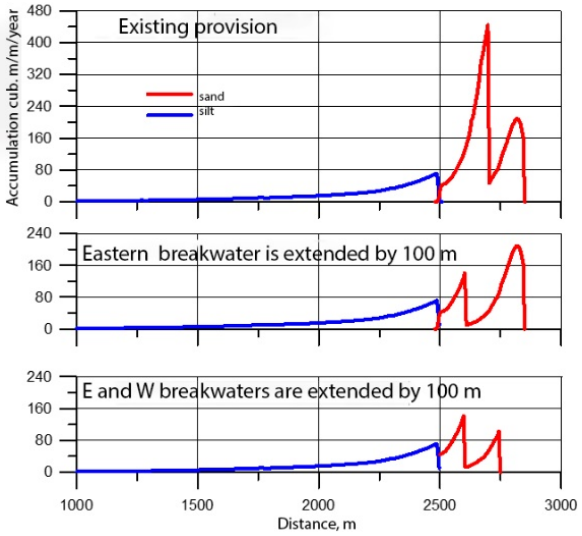

Figure 11. Comparison of the distributions of channel sedimentation volumes for different phases of breakwater extension.

3.5. Shoreline dynamics in the vicinity of the east breakwater

In order to solve the problem of the breakwater extension, it is first necessary to trace the dynamics of the shoreline in the vicinity of the structure and assess its possible future changes. The fact is that due

to the accumulation of sand in front of the breakwater, the shore gradually grows. If we compare the present position of the shoreline with the one marked on the sea maps of the 1980s, it turns out to be shifted towards the sea by about a hundred meters.

Figure 12. Shoreline changes in the area of the channel mouth from 2006 to 2019 based on the analysis of satellite images.

The coastal advance is most clearly demonstrated by satellite images taken at intervals of several years. Fig. 12 shows the changes in the shore position near the east breakwater for the period from 2006 to 2019 (the results were obtained at MGSU). The linear scale in this case can be a channel width of 100 m. The figure shows that over 13 years, the coastline has shifted toward the sea by about 40–50 m, i.e., the rate of advancement is close to 3–4 m/year.

3.6. Shore dynamics to the west of the channel

The dynamics of the shoreline area adjacent to the channel on the west side can be judged based on information obtained by analyzing satellite images taken over the past decades. The results of the shoreline changes analysis provided by MGSU are shown in Fig. 13.

First of all, it should be noted that there are no significant changes in the area in question. The shoreline fluctuates from year to year with an amplitude of about 10 m. However, its average position remains generally stable. The tendency to erosion is not detected. It is rather possible to speak about some accretion of the shore. For example, between 2003 and 2020, the west breakwater shore has moved out at a distance of about 10 m. I.e., the average advance rate over 17 years was about 0.6 m/year.

Figure 13. Shoreline changes to the west of the approach channel.

Thus, over the next 50 years, the shoreline at the west breakwater may be extended by about 30 m. However, this is unlikely to noticeably affect the protective function of the structure, the length of which, considering the planned extension, should be about 150 m.

Although there is no coastal retreat in the area considered, it is possible that there may be downstream erosion due to interruption of sediment flow after the extension of the breakwater. It should,

however, be considered that the flow is also interrupted in the present position, with the bulk of it accumulating in the channel. After the reconstruction of the breakwaters, most of the material will be retained not in the channel, but near the structures, i.e. there will be a redistribution of accumulation volumes, but the total volume of sediment deficit downstream will not change significantly. Consequently, we can expect shoreline changes to the west of the channel to continue to be insignificant.

4. Conclusions

The results of the study can be summarised as follows:

1) The sedimentation of the approach channel is determined separately for the area of predominantly sandy and the area of predominantly muddy sediments. The technique allows you to explore various scenarios of mole extension and determine the best option. The results are verified by the data of space images.

2) At present, the existing protective structures of Temryuk seaport contain a relatively small part of sand sedimentation moving along the shore: 3 thousand m^3/year for the west breakwater and 24 thousand m^3/year for the east one. The total volume of sand sedimentation into the channel reaches 50 000 m^3/year. Maximum specific sedimentation exceeds 400 $m^3m^{-1}year^{-1}$ (at the head of the east breakwater).

3) Due to the accumulation of sand in front of the east breakwater, the coastline is gradually advancing into the sea and, based on the obtained estimations, will reach the head of the existing breakwater in 25 years. In this connection, two variants of the east breakwater extension are considered: variant 1 – by 100 m, variant 2 – by 200 m.

4) If the east breakwater is extended by 100 m, the sedimentation of the channel will almost halve (from 55 to 30 thousand m^3/year). Maximum specific accumulation will decrease to 200 $m^3m^{-1}year^{-1}$.

5) If the east breakwater is extended by 200 m, the sedimentation will decrease insignificantly in comparison with the variant of extended by 100 m (from 30 to 23 thousand m^3/year), though the structure will be able to fulfil its protective function twice as long (approximately 100 years).

6) If the west breakwater is lengthened by 100 m, the sedimentation will become two times less, and the volume of sand accumulation in the channel will not exceed 15 thousand m^3/year. The maximum specific accumulation will decrease to 140 $m^3m^{-1}year^{-1}$. For a radical reduction of the channel's sanding, it is advisable to extend not only the eastern, but also the west breakwater.

7) According to the available data, the bank to the west of the channel is generally stable and will not undergo significant changes after the breakwater reconstruction. At the same time, the shoreline may be extended by about 30 m over a 50-year period at the west breakwater, which, however, will not lead to any noticeable deterioration of the protective properties of the structure.

References

1. Szmytkiewicz, M., Biegowski, J.X., Kaczmarek, L.M., Okrój, T., Ostrowski, R.X., Pruszak, Z., Różyńsky, G., Skaja, M. Coastline changes nearby harbour structures: comparative analysis of one-line models versus field data. Coastal Engineering. 2000. 40 (2). Pp. 119–139. DOI: 10.1016/S0378-3839(00)00008-9
2. El-Asmar, H.M., White, K. Changes in coastal sediment transport processes due to construction of New Damietta Harbour, Nile Delta, Egypt. Coastal Engineering. 2002. 46(2). Pp. 127–138. DOI: 10.1016/S0378-3839(02)00068-6
3. Zarifsanayei, A.R., Antolínez, J.A.A., Etemad-Shahidi, A., Cartwright, N., Strauss, D. A multi-model ensemble to investigate uncertainty in the estimation of wave-driven longshore sediment transport patterns along a non-straight coastline. Coastal Engineering. 2022. 173. Pp. 104080. DOI: 10.1016/j.coastaleng.2022.104080
4. Bergillos, R.J., Masselink, G., Ortega-Sánchez, M. Coupling cross-shore and longshore sediment transport to model storm response along a mixed sand-gravel coast under varying wave directions. Coastal Engineering. 2017. 129. Pp. 93–104. DOI: 10.1016/j.coastaleng.2017.09.009
5. Kuriyama, Y., Sakamoto, H. Cross-shore distribution of long-term average longshore sediment transport rate on a sandy beach exposed to waves with various directionalities. Coastal Engineering. 2014. 86. Pp. 27–35. DOI: 10.1016/j.coastaleng.2014.01.009
6. Sheela Nair, L., Sundar, V., Kurian, N.P. Longshore Sediment Transport along the Coast of Kerala in Southwest India. Procedia Engineering. 2015. 116 (1). Pp. 40–46. DOI: 10.1016/j.proeng.2015.08.262
7. Samaras, A.G., Koutitas, C.G. Comparison of three longshore sediment transport rate formulae in shoreline evolution modeling near stream mouths. Ocean Engineering. 2014. 92. Pp. 255–266. DOI: 10.1016/j.oceaneng.2014.10.005
8. Zhang, W., Deng, J., Harff, J., Schneider, R., Dudzinska-Nowak, J. A coupled modeling scheme for longshore sediment transport of wave-dominated coasts — A case study from the southern Baltic Sea. Coastal Engineering. 2013. 72. Pp. 39–55. DOI: 10.1016/j.coastaleng.2012.09.003
9. Goldstein, E.B., Coco, G., Plant, N.G. A review of machine learning applications to coastal sediment transport and morphodynamics. Earth-Science Reviews. 2019. 194. Pp. 97–108. DOI: 10.1016/j.earscirev.2019.04.022
10. Bosboom, J., Mol, M., Reniers, A.J.H.M., Stive, M.J.F., de Valk, C.F. Optimal sediment transport for morphodynamic model validation. Coastal Engineering. 2020. 158. Pp. 103662. DOI: 10.1016/j.coastaleng.2020.103662
11. Haas, K.A., Hanes, D.M. Process-based modeling of total longshore sediment transport. Journal of Coastal Research. 2004. 20(3). Pp. 853–861.

12. Bailard, J.A. An energetics total load sediment transport model for a plane sloping beach. Journal of Geophysical Research. 1981. 86 (C11). Pp. 10938. DOI: 10.1029/JC086iC11p10938
13. Bayram, A., Larson, M., Hanson, H. A new formula for the total longshore sediment transport rate. Coastal Engineering. 2007. 54 (9). Pp. 700–710. DOI: 10.1016/j.coastaleng.2007.04.001
14. Hanson, H., Larson, M., Kraus, N.C. Calculation of beach change under interacting cross-shore and longshore processes. Coastal Engineering. 2010. 57 (6). Pp. 610–619. DOI: 10.1016/j.coastaleng.2010.02.002
15. Hanson, H. Genesis: a generalized shoreline change numerical model. Journal of Coastal Research. 1989. 5(1). Pp. 1–27.
16. Bowen, A.J. Simple models of nearshore sedimentation; beach profiles and longshore bars. Geol. Survey of Canada. 1980. Pp. 1–11. DOI: 10.4095/102213
17. Leont'yev, I.O. Izmeneniya kontura berega, vyzvannyye poperechnym sooruzheniyem v beregovoy zone morya [Changes in shoreline contour due to cross-shore structure in the Sea Coastal Zone]. Geomorphology RAS. 2018. (3). Pp. 32–39. DOI: 10.7868/S0435428118030033
18. Eelsalu, M., Parnell, K.E., Soomere, T. Sandy beach evolution in the low-energy microtidal Baltic Sea: Attribution of changes to hydrometeorological forcing. Geomorphology. 2022. 414. Pp. 108383. DOI: 10.1016/j.geomorph.2022.108383
19. RD.31.31.47-88. Normy proyektirovaniya morskikh kanalov [Design Standards for Maritime Canals]. USSR Minmorflot 114, Moscow, 1988.
20. Leont'yev, I.O. Coastal dynamics: waves, currents, sediment transport. Moscow, GEOS, 2001. 272 p.
21. Hadla, G., Anshakov, A.S., Kantarzhi, I.G. The Role of Currents and Waves in the Movement of Sediments in the Vicinity of Coastal Hydraulic Structures. Power Technology and Engineering. 2021. 54 (6). Pp. 841–847. DOI: 10.1007/s10749-021-01297-0
22. Kantarzhi, I., Leont'yev, I., Hadla, G. Modeling of Lithodynamic Processes in the Area of a Large Navigation Channel. APAC 2019. Singapore, Springer Singapore, 2020. Pp. 441–447. DOI: 10.1007/978-981-15-0291-0_61
23. Van Wellen, E., Chadwick, A.J., Mason, T. A review and assessment of longshore sediment transport equations for coarse-grained beaches. Coastal Engineering. 2000. 40 (3). Pp. 243–275. DOI: 10.1016/S0378-3839(00)00031-4
24. Capobianco, M., Larson, M., Nicholls R.J., Kraus, N.C. Depth of closure: a contribution to the reconcillation of theory, practice and evidence. Int. Conf. Coastal Dynamics'97. Plymouth, 1997. Pp. 506–515.
25. Gladish, V.A., Logvina, E.A., Nesterov, A.V., Kubishkin, N.V. Intensity of the lithodynamical processes in the sea navigation channel Sabetta. Eng. Stud. 2017. No. 4. Pp. 36–45.
26. Van Wellen, E., Chadwick, A.J., Bird, P.A.D., Bray, M., Lee, M., Morfett, J.C. Coastal sediment transport on shingle beaches. Proceedings of Coastal Dynamics'97, American Society of Civil Engineers, 1997. Pp. 38–47.
27. Van Rijn L. Principles of sediment transport in rivers, estuaries and coastal seas. Aqua Publ. Amsterdam, 1993.
28. Rodriguez, H.N., Mehta, A.J. Longshore transport of fine-grained sediment. Continental Shelf Research. 2000. 20 (12–13). Pp. 1419–1432. DOI: 10.1016/S0278-4343(00)00030-3
29. Ghosh, L.K., Prasad, N., Joshi, V.B., Kunte, S.S. A study on siltation in access channel to a port. Coastal Engineering. 2001. 43 (1). Pp. 59–74. DOI: 10.1016/S0378-3839(01)00006-0
30. Rossiyskiy morskoy registr sudokhodstva. Spravochnyye dannyye po rezhimu vetra i volneniya Baltiyskogo, Severnogo, Chernogo, Azovskogo i Sredizemnogo morey [Russian Maritime Register of Shipping. Reference data on wind and wave regimes in the Baltic, North, Black, Azov and Mediterranean Seas]. St. Petersburg: Gidrometeoizdat, 2006. 452.

Information about authors:

Izmail Kantardgi, *Doctor of Technical Sciences*
E-mail: kantardgi@yandex.ru

Igor Leont'yev, *Doctor of Geography*
ORCID: https://orcid.org/0000-0002-5010-6239
E-mail: igor.leontiev@gmail.com

Alexander Kuprin,
ORCID: https://orcid.org/0000-0002-4186-2753
E-mail: rtyter55@gmail.com

Received 05.02.2023. Approved after reviewing 07.04.2023. Accepted 07.04.2023.